

УДК 539.12.125.4

« $\gamma + \text{Jet}$ » EVENTS RATE ESTIMATION FOR GLUON DISTRIBUTION DETERMINATION AT LHC

D.V.Bandourin, V.F.Konopliyanikov, N.B.Skachkov

It is shown that « $\gamma + \text{Jet}$ » events, being collected at LHC, would provide us with the data sufficient for an extraction of gluon distribution function in a proton using valence and sea quark distributions measured in the same experiment with another physical processes. A new region of $10^{-4} \leq x \leq 10^{-1}$ with $1.6 \cdot 10^3 \leq Q^2 \leq 10^5$ (GeV/c)² can be covered. The rates of $g c \rightarrow \gamma^{\text{dir}} + \text{Jet}$ events are also given.

The investigation has been performed at the Dzhelapov Laboratory of Nuclear Problems, JINR.

Оценка числа « $\gamma + \text{Jet}$ »-событий для определения глюонного распределения на ЛHC

Д.В.Бандурин и др.

Показано, что « $\gamma + \text{Jet}$ »-события, будучи собранными на ЛHC, обеспечат нас необходимыми данными для извлечения функции глюонного распределения в протоне при использовании распределений валентных и морских кварков, измеренных в том же самом эксперименте в других физических процессах. При этом может быть покрыта новая область $10^{-4} \leq x \leq 10^{-1}$ при $1,6 \cdot 10^3 \leq Q^2 \leq 10^5$ (ГэВ/с)². В работе также даются числа $g c \rightarrow \gamma^{\text{dir}} + \text{Jet}$ -событий.

Работа выполнена в Лаборатории ядерных проблем им. В.П.Джелепова ОИЯИ.

1. INTRODUCTION

As many of theoretical predictions for new particles (Higgs, SUSY) production at LHC are based on model estimations of gluon density behavior at low x and high Q^2 , the measurement of proton gluon density for this kinematical region directly in LHC experiments would be obviously quite useful. One of the promising channels for this measurement, as it was shown in [1], is a high P_t direct photon production $pp \rightarrow \gamma^{\text{dir}} + X$. The region of high P_t , reached up to now by UA1 [2], UA2 [3], CDF [4] and D0 [5] extends up to $P_t \approx 60$ GeV/c. These data together with the latter ones (see references in [6–13]) and recent E706 [14] and UA6 [15] results give an opportunity for tuning the form of gluon distribution (see [8, 10, 16]). The rates and estimation for cross sections of inclusive direct photon production at LHC are given in [1] (see also [17]).

Here we shall consider another process (see also [18])

$$pp \rightarrow \gamma^{\text{dir}} + 1 \text{ Jet} + X \quad (1)$$

(for experimental results see [19,20]) that at the leading order is defined by two QCD subprocesses: «Compton-like» process (which gives the main contribution) $qg \rightarrow \gamma + q$ and «annihilation» process $q\bar{q} \rightarrow \gamma + g$.

The study of $\gamma^{\text{dir}} + 1 \text{ Jet}$ final state is a more preferable one from the viewpoint of extraction of information on gluon distribution. In the case of inclusive direct photons production, the cross section is given as an integral over partons ($a, b = \text{quarks and gluon}$) distribution functions $f_a(x_a, Q^2)$, while for (1) at $P_t \geq 30 \text{ GeV}/c$ (i.e., the region where k_T smearing effects should not be important, see [11]) it is expressed directly through these distributions (see, for example, [7]; $\eta_1 = \eta^\gamma$, $\eta_2 = \eta^{\text{jet}}$; $P_t = P_t^\gamma$; $a, b = q, \bar{q}, g$; $1, 2 = q, \bar{q}, g, \gamma$)

$$\frac{d\sigma}{d\eta_1 d\eta_2 dP_t^2} = \sum_{a,b} x_a f_a(x_a, Q^2) x_b f_b(x_b, Q^2) \frac{d\sigma}{d\hat{t}}(ab \rightarrow 12), \quad (2)$$

where $x_{a,b} = P_t/\sqrt{s} \cdot (\exp(\pm\eta_1) + \exp(\pm\eta_2))$. Formula (4) with the knowledge of the results of independent measurements of q, \bar{q} distributions [18] allows one to determine gluon $f_g(x, Q^2)$ distribution.

Our work is based on the results of [25], where the selection criteria of « $\gamma + \text{Jet}$ » events with a clean topology and most suitable for jet energy absolute scale setting at LHC energy were developed. In [25] mainly PYTHIA was used complemented by GEANT simulation to study a possibility of the background events rejection. Below the CMS detector geometry will be used as an example.

2. DEFINITION OF SELECTION RULES

Our selection conditions for « $\gamma + \text{Jet}$ » events were chosen as in [25]. We suppose the ECAL size to be limited by $|\eta| \leq 2.61$ and HCAL is limited by $|\eta| \leq 5.0$ (CMS geometry), where $\eta = -\ln(\tan(\theta/2))$ is a pseudorapidity defined through a polar angle θ counted from the beam line. In the plane transverse to the beam line the azimuthal angle ϕ defines the directions of $\mathbf{P}_t^{\text{jet}}$ and \mathbf{P}_t^γ .

1. We select the events with one jet and one photon candidate with

$$P_t^\gamma \geq 40 \text{ GeV}/c; \quad P_t^{\text{jet}} \geq 30 \text{ GeV}/c. \quad (3)$$

The jet is defined here according to PYTHIA jet-finding algorithm LUCCELL. The jet cone radius R in $\eta - \phi$ space is taken as $R = ((\Delta\eta)^2 + (\Delta\phi)^2)^{1/2} = 0.7$.

2. To suppress the background processes, only the events with «isolated» photons are taken. To do this, we restrict:

a) the value of the scalar sum of P_t of hadrons and other particles surrounding a photon within a cone of $R_{\text{isol}}^\gamma = ((\Delta\eta)^2 + (\Delta\phi)^2)^{1/2} = 0.7$ («absolute isolation cut»)

$$\sum_{i \in R} P_t^i \equiv P_t^{\text{isol}} \leq P_{t\text{CUT}}^{\text{isol}}; \quad (4)$$

b) the value of a fraction («relative isolation cut»)

$$\sum_{i \in R} P_t^i / P_t^\gamma \equiv \epsilon^\gamma \leq \epsilon_{\text{CUT}}^\gamma; \quad (5)$$

c) we accept only the events having no charged tracks (particles) with $P_t > 1$ GeV/c within the R_{isol}^γ cone around the photon candidate.

3. To be consistent with the application condition of the NLO formulae, one should avoid an infrared dangerous region and take care of P_t population in the region close to a photon (see [21–24]). In accordance with [22] we also restrict the scalar sum of P_t of particles around a photon within a cone of a smaller radius $R_{\text{singl}} = 0.175 = 1/4 R_{\text{isol}}^\gamma$.

Due to this cut,

$$\sum_{i \in R_{\text{singl}}} P_t^i \equiv P_t^{\text{singl}} \leq 2 \text{ GeV}/c, \quad (i \neq \gamma - \text{dir}) \quad (6)$$

an «isolated» photon with high P_t also becomes «single» within an area of 8 towers (of 0.087×0.087 size according to CMS geometry) which surround the tower hit by it (analog of 3×3 tower window algorithm).

4. We also consider the structure of every event with the photon candidate at a more precise level of 5×5 crystal cells window (size of one CMS HCAL tower) with a cell size of 0.0175×0.0175 . To suppress the background events with photons resulting from high energetic π^0 -, η -, ω - and K_S^0 -mesons, we apply in addition the following cuts:

a) the ECAL signal can be considered as a candidate to be a direct photon if it fits inside the 3×3 ECAL crystal cell window (typical size of photon shower in ECAL found from GEANT simulation with CMSIM package) with the highest P_t of γ/e in the centre;

b) the value of a scalar sum of P_t (P_t^{sum}) of stable particles in the 5×5 crystal cell window in the region out of a smaller 3×3 crystal cell window having the cell with the direct photon candidate (i.e., with the largest P_t of γ/e) as the central one, should be restricted by 1 GeV/c, i.e.,

$$P_t^{\text{sum}} \leq 1 \text{ GeV}/c; \quad (7)$$

c) we require the absence of a high P_t hadron in this 5×5 crystal cell window (that means an imposing of an upper cut on the HCAL signal at least in the one-tower area) around the direct photon:

$$P_t^{\text{hadr}} \leq 5 \text{ GeV}/c. \quad (8)$$

We cannot reduce this value to, for example, 2–3 GeV/c, because a hadron with P_t below 2–3 GeV/c deposits most of its energy in ECAL and may not reveal itself in HCAL.

5. The events with the vector $\mathbf{P}_t^{\text{Jet}}$ being «back-to-back» to the vector \mathbf{P}_t^γ in the transverse to a beam line plane within $\Delta\phi$ which is defined by equation:

$$\phi_{(\gamma, \text{jet})} = 180^\circ \pm \Delta\phi \quad (\Delta\phi = 15^\circ, 10^\circ, 5^\circ) \quad (9)$$

(5° is a size of one CMS HCAL tower in ϕ) for the following definition of the angle $\phi_{(\gamma, \text{jet})}$:

$$\mathbf{P}_t^\gamma \mathbf{P}_t^{\text{Jet}} = P_t^\gamma P_t^{\text{Jet}} \cdot \cos(\phi_{(\gamma, \text{jet})}), \quad \text{with } P_t^\gamma = |\mathbf{P}_t^\gamma|, \quad P_t^{\text{Jet}} = |\mathbf{P}_t^{\text{Jet}}|.$$

6. To discard the background events, we choose the events that do not have any other (except one jet) minijet-like or cluster high P_t activity (taking the cluster cone $R_{\text{clust}}(\eta, \phi) = 0.7$) with the P_t^{clust} higher than some threshold $P_{\text{CUT}}^{\text{clust}}$ value. Thus we select events with

$$P_t^{\text{clust}} \leq P_{t\text{CUT}}^{\text{clust}}, \quad (10)$$

where clusters are found by the same jet-finder (LUCCELL) used to find the jet in the event.

7. We limit the value of modulus of the vector sum of \mathbf{P}_t of all particles that fit into the region covered by ECAL and HCAL except the « $\gamma + \text{Jet}$ » system (i.e., the cells «out of the jet and photon» regions):

$$\left| \sum_{i \notin \text{jet}, \gamma\text{-dir}} \mathbf{P}_t^i \right| \equiv P_t^{\text{out}} \leq P_{t\text{CUT}}^{\text{out}}, \quad |\eta| < 5. \quad (11)$$

8. To reduce the value of P_t^{Jet} uncertainty due to possible presence of the neutrino contribution to a jet and to diminish background events with high energetic electrons [25], we select only events with a small P_t^{miss} value:

$$P_t^{\text{miss}} \leq P_{t\text{CUT}}^{\text{miss}}. \quad (12)$$

9. In addition to selection cuts 1–8 one more new object, named an «isolated jet», will be introduced. To do this, we also involve a new requirement of «jet isolation», i.e., the presence of a «clean enough» (in the sense of small P_t activity) region inside the ring (of $\Delta R = 0.3$ size) around the jet. Following this picture we restrict the value of the ratio of scalar sum of particles transverse momenta belonging to this ring, i.e.,

$$P_t^{\text{ring}} / P_t^\gamma \equiv \epsilon^{\text{jet}} \leq 2\%, \quad \text{where} \quad P_t^{\text{ring}} = \sum_{i \in 0.7 < R < 1} |\mathbf{P}_t^i|. \quad (13)$$

The exact values of cut parameters, i.e., $P_{t\text{CUT}}^{\text{isol}}$, $\epsilon_{\text{CUT}}^\gamma$, ϵ^{jet} , $P_{t\text{CUT}}^{\text{clust}}$, $P_{t\text{CUT}}^{\text{out}}$, will be specified bellow since they may be different, for instance, for various P_t^γ intervals (more loose for higher P_t^γ).

Three criteria, 6, 7, and 9, are new and have not been used in previous experiments. Their efficiency, as well as an efficiency of other selection criteria from the list above to reduce the background, was demonstrated in detail in papers [25], where to we refer a reader for more information.

3. BACKGROUND SUPPRESSION

To estimate the background for the signal events, we have done a simulation basing on PYTHIA 5.7 (default CTEQ2L parametrization of structure functions is used here) of a mixture of all existing in PYTHIA QCD and SM subprocesses with large cross sections (namely, 11–20, 28–31, 53, 68) together with our subprocesses (2) and (3) (14 and 29 in PYTHIA). Three generations (each of $50 \cdot 10^6$ events) with different values of minimal P_t of hard process $\hat{p}_\perp^{\text{min}}$ (CKIN(3) parameter in PYTHIA) were done. The first one is with $\hat{p}_\perp^{\text{min}} = 40$ GeV/c, the second one is with $\hat{p}_\perp^{\text{min}} = 100$ GeV/c and the third — with $\hat{p}_\perp^{\text{min}} = 200$ GeV/c. The produced photons were classified according to their origin, i.e., those that are direct ones and those that result due to the radiation from quarks (denoted as « $\gamma - \text{brem}$ ») and from η -, ω -, K_S^0 -meson decays (« $\gamma - \text{mes}$ »). Another sort of background is formed by electrons e^\pm 's. However, we also should take into account the real behavior of processes in the detectors.

Table 1. Number of signal and background events remained after cuts

\hat{p}_\perp^{\min} (GeV/c)	Cuts	γ direct	γ brem	Photons from the mesons				e^\pm
				π^0	η	ω	K_S^0	
40	Preselected	7795	12951	104919	41845	10984	15058	4204
	After cuts	464	43	15	0	0	0	0
	+ jet isol.	109	7	2	0	0	0	0
100	Preselected	19359	90022	658981	247644	69210	85568	47061
	After cuts	1061	31	9	0	0	0	3
	+ jet isol.	615	14	4	0	0	0	2
200	Preselected	32629	207370	780190	288772	82477	98015	89714
	After cuts	967	16	2	0	0	0	2
	+ jet isol.	825	14	1	0	0	0	1

Table 2. Efficiencies and significance values in events without jet isolation cut (II)

\hat{p}_\perp^{\min} (GeV/c)	S	B	Eff $_S$ (%)	Eff $_B$ (%)	S/B	S/\sqrt{B}
40	464	58	5.95 ± 0.28	0.031 ± 0.004	8.0	60.9
100	1061	43	5.48 ± 0.17	0.004 ± 0.001	24.7	161.8
200	967	20	2.96 ± 0.10	0.002 ± 0.000	48.4	216.2

Table 3. Efficiencies and significance values in events with jet isolation cut (II)

\hat{p}_\perp^{\min} (GeV/c)	S	B	Eff $_S$ (%)	Eff $_B$ (%)	S/B	S/\sqrt{B}
40	109	9	1.40 ± 0.13	0.005 ± 0.002	12.1	36.3
100	615	20	3.18 ± 0.13	0.003 ± 0.000	30.8	137.5
200	825	16	2.53 ± 0.09	0.002 ± 0.000	51.6	206.3

For this aim we have performed a detailed study (based on CMSIM GEANT simulation using 5000 generated decays of each source meson) of difference between ECAL profiles of photon showers from mesons and those from direct photons for $P_t^\gamma = 40 \div 100$ GeV/c. It is shown that the suppression factor of η -, ω -, K_S^0 -mesons larger than 0.90 can be achieved with a selection efficiency of single photons taken as 90%. As for the photons from π^0 decays, the analogous estimations of the rejection factors were done for the Endcap [27,28] and Barrel [26,28] CMS ECAL regions. They are of the order of 0.20–0.70 for Barrel and 0.51–0.75 for Endcap, depending on P_t^γ and a bit on η^γ , for the same single photon selection efficiency 90%. Following [29], for our estimation needs we accept the electron track finding efficiency to be, on the average, equal to 85% for $P_t^e \geq 40$ GeV/c, neglecting its η dependence. The number of events, selected after cuts 1–9 is presented in Table 1 (with an account of the rejection efficiencies given above) separately for signal direct photon events and those caused by the background photons and electrons e^\pm . Here the line «Preselected» corresponds to the following set of cuts:

$$P_t^\gamma \geq 40 \text{ GeV}/c, \quad |\eta^\gamma| \leq 2.61, \quad P_t^{\text{jet}} \geq 30 \text{ GeV}/c, \quad P_t^{\text{hadr}} < 5 \text{ GeV}/c, \quad (14)$$

according to selection rules (1), (3a). The line «After cuts» contains the number of signal and background events after selection cuts 1–8 with the values of cuts chosen as (in addition to those in point «Preselected»):

$$P_{t\text{CUT}}^{\text{isol}} = 2 \text{ GeV}/c, \quad \epsilon_{\text{CUT}}^\gamma = 5\%, \quad \Delta\phi = 15^\circ, \quad P_{t\text{CUT}}^{\text{clust}} = 10 \text{ GeV}/c, \quad P_{t\text{CUT}}^{\text{out}} = 10 \text{ GeV}/c. \quad (15)$$

The line «+jet isolation» corresponds to the complementary cut 9 of the previous section.

The corresponding efficiencies and significance are presented in Tables 2 and 3. In these Tables the column $S(B)$ contains the number of signal (background) events with the account of the efficiencies described above. $\text{Eff}_{S(B)}$ includes the values of cut efficiencies* and their errors.

From Table 2 it is seen that ratio S/B grows while the P_t^γ value growing from 8.0 at $P_t^\gamma \geq 40 \text{ GeV}/c$ up to 48.4 at $P_t^\gamma \geq 200 \text{ GeV}/c$. The jet isolation requirement (Table 3) sufficiently improves the situation at low P_t . In that case S/B changes up to 12.1 at $P_t^\gamma \geq 40 \text{ GeV}/c$ (and up to 30.8 at $P_t^\gamma \geq 100 \text{ GeV}/c$). As is also seen from Tables 1 and 2 the background events admixture becomes nonessential for $P_t^\gamma \geq 100 \text{ GeV}/c$.

The dependence of the number of events and S/B ratio on two the most powerful cuts $P_{t\text{CUT}}^{\text{out}}$ and $P_{t\text{CUT}}^{\text{clust}}$ were studied in [25].

In Table 4 the percentage of «Compton-like» process $qg \rightarrow \gamma + q$ (as the dominant contribution comparing with «annihilation» process $q\bar{q} \rightarrow \gamma + g$) events selected with conditions 1–6 ($P_{t\text{CUT}}^{\text{clust}} = 10 \text{ GeV}/c$) is shown for different P_t^γ and η intervals: Barrel (HB) part ($|\eta| < 1.4$) and Endcap+Forward (HE+HF) part ($1.4 < |\eta| < 5.0$).

Table 4

Calorimeter part	P_t^{Jet} interval (GeV/c)		
	40–50	100–120	200–240
HB	89	84	78
HE+HF	86	82	74

The rates of only $qg \rightarrow \gamma + q$ events selected with conditions 1–9 are presented for integrated luminosity $L = 100 \text{ pb}^{-1}$ (one day of data taking at low luminosity $L = 10^{33} \text{ cm}^{-2} \cdot \text{s}^{-1}$) in Table 5 for different intervals of P_t^γ and parton x values.

Cut conditions 1–9, as it was shown in [25], allow one to select the events with a good P_t^γ and P_t^{Jet} balance because they effectively provide a good initial and final state radiation suppression, i.e., suppression of the next-to-leading order diagrams.

Table 6 gives analogous values of distribution of the number of events in the process with a charm quark [31,30] $gc \rightarrow \gamma^{\text{dir}} + c$. For these tables $P_{t\text{CUT}}^{\text{clust}}$ was fixed to be 5 GeV/c;

*Taken as a ratio of the number of signal S (background B) events, that survived cuts 1–8 or 1–9 from Section 2, to the number of the preselected events.

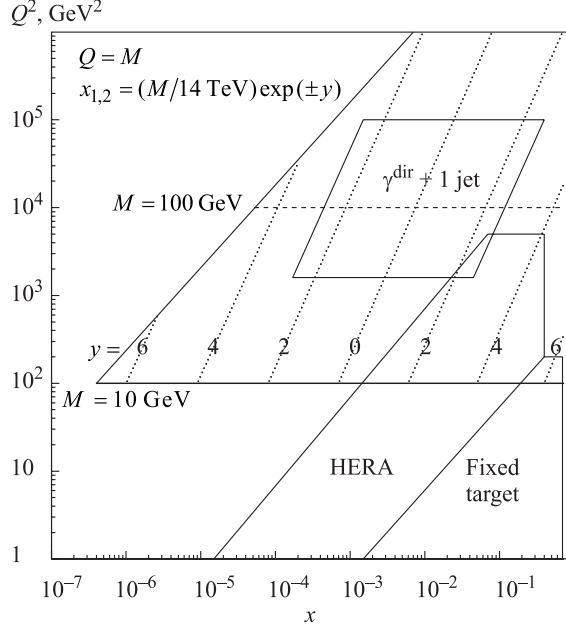


Fig. 1. LHC (x, Q^2) kinematical region for $pp \rightarrow \gamma + \text{Jet}$ process

P_t^{out} was not limited. All other cuts were put as in points 1–8 of Section 2 and with cut parameter values given by 14 and 15. The simulation of the process $gb \rightarrow \gamma^{\text{dir}} + b$ has shown that for b quark the rates are by 8–10 times smaller than those for c quark.

Figure 1 shows in the widely used (x, Q^2) kinematical plot (see [32] and also in [11]) what area can be covered by studying the process $qg \rightarrow \gamma + q$. The distribution of events inside this area is given in Table 5. From Fig. 1 and Table 5 it becomes clear that even at low LHC luminosity it would be possible to study the gluon distribution on a good statistics of « $\gamma + \text{Jet}$ » events in the region of small x at values of Q^2 that are about 2–3 orders of magnitude higher than those reached at HERA now. It is worth emphasizing that an extension of experimentally reachable region at LHC to the region of lower values of Q^2 , overlapping with the area covered by HERA, would be also of a big interest.

4. SUMMARY

It is shown that the sample of « $\gamma + \text{Jet}$ » events with a clean topology, which is most suitable for jet energy absolute scale setting at LHC energy (selected with the cut conditions of [25] that powerfully suppress initial and final state radiation, i.e., next-to-leading order diagrams contribution), covers the kinematical region of x values as small as accessible at HERA [33,34], but at much higher Q^2 values (2–3 orders of magnitude): $10^{-4} \leq x \leq 10^{-1}$ with $1.6 \cdot 10^3 \leq Q^2 \leq 10^5$ (GeV/c)². It is shown that percentage of gluon dominated subprocess $qg \rightarrow \gamma + q$ events is about 75–90% among « $\gamma + \text{Jet}$ » events what would allow, in principle, a good extraction of gluon distribution function from future LHC « $\gamma + \text{Jet}$ » data.

Table 5. Number of $gq \rightarrow \gamma^{\text{dir}} + q$ events at different Q^2 and x values for $L_{\text{int}} = 100 \text{ pb}^{-1}$

Q^2 (GeV/c) ²	x values of a parton					P_t^γ (GeV/c)
	10^{-4} – 10^{-3}	10^{-3} – 10^{-2}	10^{-2} – 10^{-1}	10^{-1} – 10^0	All x 10^{-4} – 10^0	
1600–2500	3105±104	9715±186	9243±183	941±60	23004	40–50
2500–5000	1217±52	5539±100	5794±102	930±36	13481	50–71
5000–10000	144±9	1502±29	1671±30	407±14	3724	71–100
10000–20000	6±1	328±8	422±9	161±5	916	100–141
20000–40000	0	65±2	102±2	52±2	219	141–200
40000–80000	0	9±1	18±1	11±1	37	200–283

Table 6. Number of $gc \rightarrow \gamma^{\text{dir}} + c$ events at different Q^2 and x values for $L_{\text{int}} = 100 \text{ pb}^{-1}$

Q^2 (GeV/c) ²	x values for c -quark					P_t^γ (GeV/c)
	10^{-4} – 10^{-3}	10^{-3} – 10^{-2}	10^{-2} – 10^{-1}	10^{-1} – 10^0	All x 10^{-4} – 10^0	
1600–2500	426±39	1395±71	1495±73	161±24	3477	40–50
2500–5000	155±18	806±39	841±39	86±11	1888	50–71
5000–10000	18±3	214±11	244±12	50±5	526	71–100
10000–20000	1±1	37±3	51±3	17±2	106	100–141
20000–40000	0	6±1	14±1	4±0.3	24	141–200
40000–80000	0	1±0.2	2±0.2	1±0.2	4	200–283

Acknowledgements. We thank P. Aurenche, D. Denegri, M. Dittmar, M. Fontannaz, J.Ph. Guillet, M.L. Mangano, E. Pilon, and S. Tapprogge for helpful discussions.

References

1. Aurenche P. et al. — Proc. of «ECFA LHC Workshop», Aachen, Germany, 4–9 Oktob. 1990, edited by G. Jarlskog and D. Rein (CERN-Report No.90–10, Geneva, Switzerland, 1990), v.II.
2. UA1 Collaboration, Albajar C. et al. — Phys. Lett., 1998, v.209B, p.385.
3. UA2 Collaboration, Ansari R. et al. — Phys. Lett., 1989, v.176B, p.239.
4. CDF Collaboration. Abe F. et al. — Phys. Rev. Lett., 1992, v.68, p.2734;
Abe F. et al. — Phys. Rev., 1993, v.D48, p.2998;
Abe F. et al. — Phys. Rev. Lett., 1994, v.73, p.2662.
5. D0 Collaboration, Abachi F. et al. — Phys. Rev. Lett., 1996, v.77, p.5011.
6. Ferbel T., Molzon W.R. — Rev. Mod. Phys., 1984, v.56, p.181.
7. Owens J.F. — Rev. Mod. Phys., 1987, v.59, p.465.

8. Aurenche P. et al. — Phys. Rev., 1989, v.D39, p.3275.
9. Huston J. et al. — Phys. Rev., 1995, v.D51, p.6139.
10. Vogelsang W., Vogt A. — Nucl. Phys., 1995, v.B453, p.334.
11. Huston J. — ATLAS Note ATL-Phys-99-008, CERN, 1999.
12. Vogelsang W., Whally M. — J. Phys., 1997, v.G23, p.A1.
13. Frixione S., Vogelsang W. — CERN-TH/99-247 hep-ph/9908387.
14. E706 Collaboration, Apanasevich L. et al. — Phys. Rev. Lett., 1997, v.81, p.2642.
15. UA6 Collaboration, Balocchi G. et al. — Phys. Lett., 1998, v.B436 p.222.
16. Martin A.D. et al. — Eur. Phys. J., 1998, v.C4, p.463.
17. Aurenche P., Fontannaz M., Frixione S. — Proc. of «CERN Workshop on Standard Model Physics (and more) at the LHC», QCD, Section 6.1 «General Features of Photon Production», Yellow Report CERN-2000-004, 9 May 2000, CERN, Geneva.
18. Dittmar M., Pauss F., Zurcher D. — Phys. Rev., 1997, v.D56, p.7284-7290.
19. CDF Collaboration, Abe F. et al. — Phys. Rev., 1998, v.D57, p.1359;
ISR-AFS Collaboration, Akesson T. et al. — Zeit. Phys., 1987, v.C34, p.293.
20. CDF Collaboration, Abe F. et al. — Phys. Rev., 1998, v.D57, p.67.
21. Berger E.L., Qiu J. — Phys. Rev., 1991, v.D44, p.2002.
22. Frixione S. — Phys. Lett., 1998, v.B429, p.369.
23. Catani S., Fontannaz M., Pilon E. — Phys. Rev., 1998, v.D58, p.094025.
24. Fontannaz M., Frixione S., Tapprogge S. — Proc. of «CERN Workshop on Standard Model Physics (and more) at the LHC», QCD, Section 6 «Prompt Photon Production», Yellow Report CERN-2000-004, 9 May 2000, CERN, Geneva.
25. Bandourin D.V., Konoplyanikov V.F., Skachkov N.B. — Jet Energy Scale Setting with « $\gamma + \text{Jet}$ » Events at LHC Energies. JINR Preprints E2-2000-251, E2-2000-255, Dubna, 2000.
26. Borissov L. et al. — CMS-Note 1997/050.
27. Barney D. et al. — CMS-Note 1998/088.
28. CMS Electromagnetic Calorimeter Project, Technical Design Report, CERN/LHCC 97-33, CMS TDR 4, p.326.
29. CMS Tracker Project, Technical Design Report, CERN/LHCC 98-6, CMS TDR 5, p.488.
30. Dittmar M., Mazumdar K. — «The Possibility to Measure the Charm, Beauty and Strange Quark Luminosity at the LHC», CMS Note in preparation.

31. Dittmar M., Mazumdar K., Skachkov N. — Proc. of «CERN Workshop on Standard Model Physics (and more) at the LHC», QCD, Section 2.7 «Measuring Parton Luminosities ...», Yellow Report CERN-2000-004, 9 May 2000, CERN, Geneva.
32. Ball R., Dittmar M., Stirling W.J. — Proc. of «CERN Workshop on Standard Model Physics (and more) at the LHC», QCD, Section 2 «Parton Distribution Functions», Yellow Report CERN-2000-004, 9 May 2000, CERN, Geneva.
33. H1 Collaboration, Aid S. et al. — Nucl. Phys., 1996, v.B470, p.3;
Adloff C. et al. — Nucl. Phys., 1997, v.B497, p.3.
34. ZEUS Collaboration, Derrick M. et al. — Zeit. Phys., 1996, v.C69, p.607;
Derrick M. et al. — Zeit. Phys., 1996, v.C72, p.399.

Received on November 30, 2000.